

Ping-pong ball cannon: Why do barrel and balls fly in the same direction?

Thorsten Pöschel and Daniel S. Nasato

Institute for Multiscale Simulations, Friedrich-Alexander-Universität Erlangen-Nürnberg, Erlangen 91058, Germany

Eric J. R. Parteli

Department of Geosciences, University of Cologne, Pohligstraße 3, 50969 Cologne, Germany

Jason A. C. Gallas

Institute for Multiscale Simulations, Friedrich-Alexander-Universität Erlangen-Nürnberg, Erlangen 91058, Germany; Max-Planck-Institut für Physik komplexer Systeme, D-01187 Dresden, Germany; Instituto de Altos Estudos da Paraíba, Rua Silvino Lopes 419-2502, 58039-190 João Pessoa, Brazil; and Complexity Sciences Center, 9225 Collins Avenue Suite 1208, Surfside, Florida 33154

Patric Müller

Institute for Multiscale Simulations, Friedrich-Alexander-Universität Erlangen-Nürnberg, Erlangen 91058, Germany

(Received 18 August 2018; accepted 13 January 2019)

An impressive ping-pong ball cannon can be made by placing a bottle of liquid nitrogen at the bottom of a container and quickly covering it with, say, 1500 ping-pong balls. The liquid turns rapidly into a gas whose mounting pressure explodes the bottle, sending a swarm of balls upward out of the container. Surprisingly, the container also moves upward. This is a counterintuitive effect because the balance of forces, that is, Newton's third law does not seem to allow the container to move upwards. We explain the effect as a consequence of granular jamming in combination with Coulomb's friction law. © 2019 American Association of Physics Teachers.

<https://doi.org/10.1119/1.5088805>

I. INTRODUCTION

A startling classroom experiment presently attracting much attention involves firing a so-called liquid nitrogen ping-pong ball cannon. This spectacular experiment is frequently performed in front of different audiences and may be seen in several science TV shows, e.g., Ref. 1. The experiment captivates the interest of students and seems to motivate them to learn science.

The internet contains many videos of the ping-pong ball cannon experiment, under different conditions, e.g., Refs. 2 and 3. A snapshot taken from such an experiment, performed at the University of Plymouth, UK, is shown in Fig. 1. In this figure, one sees ping-pong balls being shot out of a flying barrel. The ping-pong ball cannon is a simple device to demonstrate the explosive power of expanding gases.

Basically, the ping-pong ball cannon is made by placing a common two-liter plastic bottle partially filled with about 0.5 l of liquid nitrogen at the bottom of a metallic or plastic container. The aperture of the nitrogen bottle is closed, the bottle is placed inside the container, and then covered quickly by some 1500 ping-pong balls. It is also usual to add some water at the bottom of the container to accelerate the conversion of the nitrogen from the liquid to the gas state. After a few seconds, the mounting pressure of the rapidly expanding gas inside the sealed bottle provokes the bottle to explode, throwing the ping-pong balls out of the barrel, to the amusement of the audience (Fig. 1).

Apart from the great fun for the audiences, there is a physical question which in our opinion deserves closer consideration, namely, why do the container and the balls jump off the floor in the same direction immediately after the explosion? At a first glance, this is a counterintuitive behavior because when the ping-pong balls are accelerated upwards,

due to a certain force one should expect the barrel to be subjected to a downward force, according to Newton's third law: *To every force, there is always a counterforce: the forces are always of equal magnitude and act in opposite directions.*⁴ Obviously, there is a force accelerating the balls upwards. Consequently, there should be a corresponding counter-force, directed downwards. Such a force would, however, simply increase the apparent weight of the barrel pressing it harder into the solid floor. According to this argument, of course, the force due to the explosion would not push the container up, but would press it down. So, a natural question is to ask what exactly is making the barrel to jump up over 1 m off the ground?

The ubiquity of videos displaying the aforementioned counterintuitive behavior of the ping-pong ball cannon provoked extensive discussions on several science boards on the internet. However, in our opinion, none of the arguments presented so far is physically reasonable. Here are samples of such arguments:

- (a) "The bottom of the garbage can is slightly concave,...so that only the lip around the bottom contacts with the ground. The sudden expansion of gas punched the bottom out so for a moment it was convex, launching the can up into the air."⁵
- (b) "The explosion drives everything out of the bucket, leaving a partial vacuum behind, so the atmospheric pressure outside the bucket pushes it up before air rushes back in to equalize the pressure."⁶
- (c) "The bottle of liquid nitrogen was floating on top of the water. When exploding, it sent the ping pong balls up, and the water and the bottom of the container down. After a small fraction of a second the water and container could no longer go down, so it bounced up."⁷



Fig. 1. Snapshot of the experiment performed by Roy Lowry, taken from a video recording (Ref. 3). The garbage can clearly jumps off the floor, in an apparent violation of Newton's third law which requires balance of upwards and downwards forces.

While in principle, all of the above mechanisms could cause the barrel to move upwards under certain conditions, there is clear evidence that none of them is essential for the effect: Regarding argument (a), experiments were conducted with metallic barrels¹ whose bottoms would not touch the floor, even if slightly deformed. Nevertheless, the barrel lifted up in these cases. If the explosion would cause a vacuum as it is required for mechanism (b), the barrel would indeed move upwards due to the resulting pressure gradient. However, we do not see any reason why the explosion should cause a vacuum. The explosion takes place because of the rapidly expanding nitrogen gas. Therefore, the ejected air is replaced by nitrogen of similar density and, thus, no vacuum is created. Moreover, if vacuum would be the driving force, the ping-pong balls would be irrelevant for the process. Similar experiments without ping-pong balls do not show, however, any sign of motion of the barrel.^{8–10} Mechanism (c) requires the barrel to move downwards initially and to rebound at the floor later. Of course this rebound trivially leads to an upward motion of the barrel. However, this process would require the barrel to be located above the floor initially, which is obviously not the case in all experimental realizations. Indeed, the initial distance to the ground could be replaced by an elastic floor which acts like a spring that is first compressed by the downward motion of the barrel and then lifts the barrel due to its relaxation. However all available experiments were conducted on very rigid flooring where these arguments are not applicable. Further, experiments were also performed without the water required by mechanism (c).¹¹ The water only accelerates the boiling of the liquid nitrogen and renders the time between the preparation of the experiment and the explosion more predictable. In summary, none of the aforementioned arguments serve as convincing explanations of the ping-pong ball canon effect.

In yet another post, we read “The 1500 ping pong balls are irrelevant for the experiment but they serve for an impressive appearance.”¹² Quite on the contrary, in the present article we argue that the ping-pong balls are the key players that make the barrel jump along with the balls. Detailed evidence obtained from numerical simulations shows that the nitrogen volume explosion produces a *jamming effect*^{13–15} of the

outflow of ping-pong balls, thereby providing a transfer of large horizontal forces to the barrel so that the upwards motion of the balls exerts effectively a large vertical friction force on the barrel, dragging it upwards.

II. JAMMING IN GRANULAR PIPE FLOW

Before discussing the physics of the ping-pong ball canon, let us first consider another experiment, namely, the dynamics of the flow of dry granular matter through a vertical pipe: At low density, granular matter flows similarly to ordinary fluids at approximately homogeneous density. At larger density, however, a sudden increase (ideally a divergence) of the viscosity of the granular fluid is frequently observed. Due to the increased viscosity, the material is able to sustain large shear forces, which enable the formation of plugs in which the relative motion among the individual particles is arrested and the granulate behaves like a solid. This process is called jamming and the corresponding state of a granulate is called a jammed state. In ordinary systems, friction between the grains is essential for jamming. In narrow systems, where the size of the confinement is comparable to the particle size, however, jamming may occur even in the case of ideally smooth spheres which interact frictionlessly. If a granulate in the jammed state is loaded with a force, the resulting stresses are not homogeneous as in ordinary solids. Instead, the load is sustained locally by isolated chain-like sets of contacting grains. These particle sets are called force chains. The force chains can be seen as the edges of a force network in which the load is carried by the edges while the network cells are regions of low stress. Figure 2 illustrates this phenomenon.

The transition between the fluid state and the jammed state can be seen, e.g., in granular hopper flow:^{17–19} Granular material may pour out of the orifice of a hopper for a rather long time at nearly constant rate. However, the flow may become suddenly clogged when an arc of grains, a sort of bridge, is formed at the orifice. In this circumstance the flow stops, that is, the material is jammed. In the jammed state, the material is still structurally disordered. However, unlike a fluid it has a yield stress.²⁰ Transitions between fluid and jammed states are commonly observed in granular systems

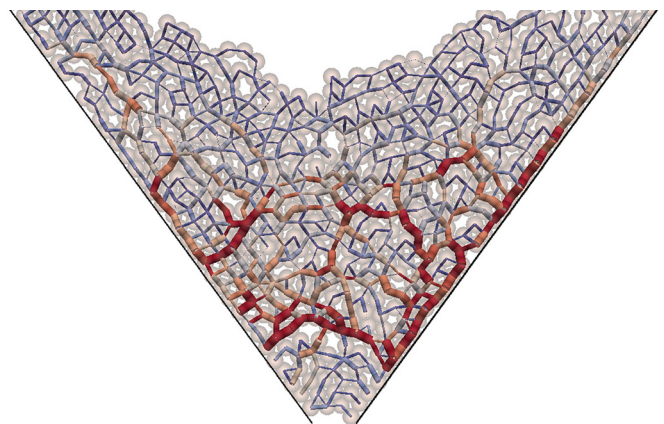


Fig. 2. Numerical DEM simulation of a clogged hopper. Particles are translucent for better visualization of the force chains. The color/widths of the joints indicates small (blue/thin) and large (red/fat) normal force of the particle in contact. Near the outflow region the force chains form arc-like structures. These structures sustain the weight of the particles in the hopper, leading to hopper clogging.

and are the distinctive signature that distinguishes granular materials from other types of matter such as gases, fluids or solids. Currently, jamming and the jamming transition are among the most intensively studied phenomena in granular matter research, e.g., Refs. 21–25.

A system of particular interest is granular flow through narrow pipes, where one observes recurrent plugs that emerge through self-organized jamming and de-jamming, see Fig. 3. When grains pour in a vertical pipe at low density, the flow is homogeneous. Essentially, the particles fall in a nearly isolated way, suffering occasional collisions with the wall and with each other. Small asperities of the pipe suddenly decrease the grains' vertical velocity and, thus, cause a horizontal velocity component which leads to subsequent collisions with the opposite wall of the pipe and with other particles. The faster the particles move, the larger their horizontal component and thus, the larger the subsequent collision frequency. As a consequence, the homogeneous flow becomes unstable and pronounced clusters of grains develop. This mechanism leads to the situation shown in Fig. 3: High-velocity particles hit the top side of a cluster such that their vertical motion slows down or even ceases. The resulting forces acting on the top of a plug are partially converted into forces acting normal to the pipe walls which enables the particles to develop a vertical friction force to the pipe walls—the particles constituting a plug cannot move collectively and the plug's motion relative to the pipe ceases. Since further material continues to enter the plug from above, the plug may apparently move slowly upwards or downwards depending on the residual motion, relative to the pipe wall,



Fig. 3. Recurrent plug formation of granular matter flowing through a narrow pipe (Ref. 16).

of the particles constituting the cluster. At the bottom of the plug, particles start to accelerate again due to gravity, and hence the plug dissolves at its lower end. The balance of these two mechanisms leads eventually to plug flow shown in Fig. 3. A theoretical approach based on these arguments²⁶ could reproduce the inhomogeneous flow observed in pipes in a satisfactory manner.

It is known that plug flow in pipes is influenced by ambient air,^{27,28} however, direct particle simulations (DEM) show that even without the influence of air the homogeneous flow of granular material through pipes is unstable and recurrent plugs appear.^{16,29} In industrial applications, the inhomogeneous flow through pipes is frequently undesired and methods to homogenize the flow have been developed, e.g., by application of certain well defined structures in the interior of the pipe, in order to avoid single particles from assuming high vertical velocity.³⁰

The motion of granular material in a vertical pipe under the action of gravity is related to the situation one encounters in the ping-pong cannon, where the granular material (the ping-pong balls) is accelerated upwards by the rapidly expanding gas. Thus, the process of plug formation and jamming in vertical pipes has its counterpart in the experiment considered in this article. In the cannon, particles are scattered by asperities of the side walls resulting eventually in a plug of ping-pong balls which is pressed against the walls of the barrel. The vertical force, F_t , exerted by an upwards-moving particle pressed by the normal force, F_n , against the wall of the barrel is limited by Coulomb's law of friction

$$F_t \leq \mu F_n, \quad (1)$$

where μ denotes the friction coefficient. When the balls are accelerated upwards by the expanding gas, the total resulting vertical force may exceed gravity causing the barrel to jump upwards. Thus, the barrel's motion results from the interplay of jamming and friction. The snapshots shown in Fig. 4 are a

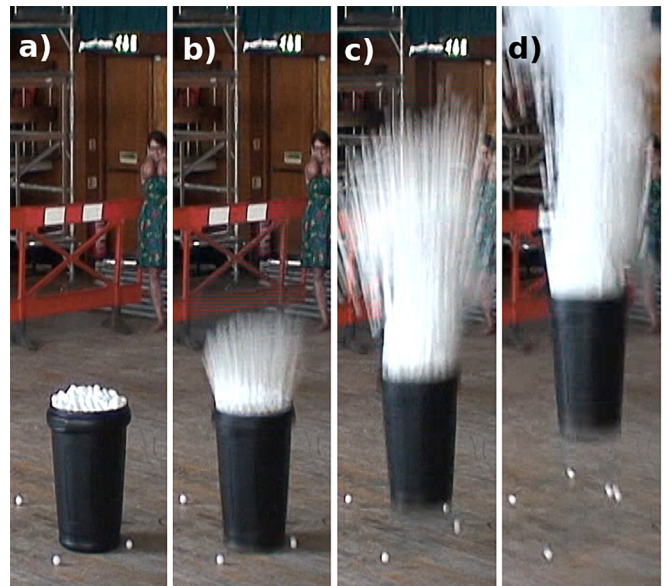


Fig. 4. Snapshots from the experiment, taken from Ref. 31. The left image shows the barrel just before the explosion. The sequence shows snapshots with time increment 1/30 s. We see that the barrel becomes airborne at the same instant when the granular packing leaves the barrel in a plug-like formation, supporting our hypothesis for the explanation of the effect.

first support of this hypothesis. In Sec. III, we substantiate this qualitative argument by means of numerical simulations. In particular, our explanation implies that an ideally smooth barrel ($\mu=0$) could not jump, because no vertical friction force could appear in this case. That this is indeed the case is verified in Sec. IV.

III. NUMERICAL SIMULATIONS

Our hypothesis concerning the physics of the flying barrel effect formulated in Sec. II relies essentially on two claims: (i) jamming of the ping-pong balls is necessary for the barrel to jump and (ii) the friction force between the upward-moving jammed plug and the barrel drags the barrel upwards. In the following, we provide numerical evidence corroborating these arguments.

We study the ping-pong ball cannon by means of numerical simulations, that is, by simultaneously integrating Newton's equations of motion for the barrel and the balls under the action of gravity. The ping-pong balls are modeled as viscoelastic spheres of mass $m=2.7$ g, and diameter $d=4$ cm, Young's modulus $Y=1.5$ GPa. A cylindrical barrel of height 80 cm, diameter 50 cm, and weight 1.7 kg is modeled with $Y=3.2$ GPa. For the Poisson ratio and the coefficient of friction between the balls and between the balls and the barrel, we assume $\nu=0.4$ and $\mu=0.8$, respectively, while for the coefficient of restitution we assume $e=0.9$. The details of the numerical model are described in the Appendix.

The explosion of the bottle filled by liquid nitrogen is a highly dynamic process which may be simulated in a number of ways. For computational convenience, we model the explosion by a sudden extrusion of the ping-pong balls; a more detailed description of the explosion process is not relevant in the context of this work. In our simulations, therefore, we describe the explosion by means of a layer of five particles which have the same properties as the particles simulating the ping-pong balls except that, at the instant of the explosion, within an interval of 5×10^{-4} s, their volumes grow by a factor 16.6, thus, pushing the ping-pong balls away. The numerical value of the expansion factor was chosen due to the best agreement of experiment and simulation for the barrel's maximum height after the explosion. The time step used in the numerical simulations is 1×10^{-8} s. The explosion is modeled as a rapid but continuous linear expansion of the 5 particles during 5×10^{-4} s, or 5×10^4 s simulation time steps. The configuration of the system before and after the explosion is shown in Fig. 5.

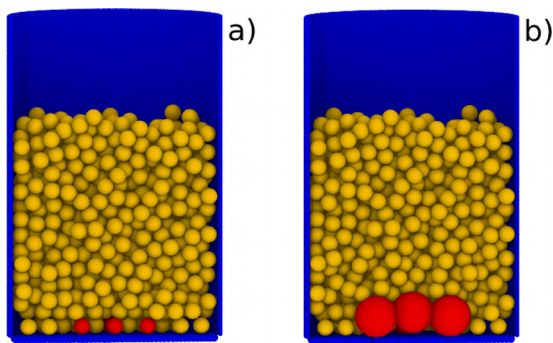


Fig. 5. Simulation of the liquid nitrogen volume explosion. (a) Cut at time $t=0$ through the barrel; (b) same at $t=5 \times 10^{-4}$ s, when the expanding particles are fully inflated to model the explosion.

Figure 6 illustrates the representative stages of firing the ping-pong ball cannon. Complementing this figure, Fig. 7 shows details of the jamming process, represented by the evolution of the force network among the ping-pong balls. Here, the center of each particle experiencing a contact force from one of its neighbors or from the wall is connected by a link whose color represents the magnitude of the force in shear direction, that is, in the direction of the contact plane. Initially (Fig. 7(a)), the forces are very small due to the action of gravity. The explosion at $t=0$ close to the bottom of the barrel causes a shock wave propagating rapidly upwards, indicated by many red colored links, see Fig. 7(b) at $t=500 \mu\text{s}$. The corresponding forces in the negative z -direction reach the bottom immediately after the explosion and are balanced by the solid floor. The emerging plug of particles, thus, generates large normal forces to the vertical wall of the barrel which allows the rapidly upward-moving plug to drag the barrel upwards, due to the friction. Starting at time $t \approx 650 \mu\text{s}$ when the shock arrives at the top layer of particles, see Fig. 7(c), the ping-pong balls leave the barrel and the plug decays. Correspondingly, the force network ceases, see Fig. 7(d) ($t=1.1$ ms).

Figure 8 shows the time averaged forces (force density), applied by the abundance of particles onto the barrel in vertical direction, thus accelerating the barrel upwards, while Fig. 9 (red line) shows the vertical velocity of the barrel as a function of time. Each data point in Fig. 8, attributed to a certain vertical position, z , and a certain time, t , shows the sum of the vertical components of all forces applied by particles located at $z \pm 0.125$ m, averaged over the interval $t \pm 125 \mu\text{s}$. From the results shown in Figs. 7 and 8, we infer the following scenario: In the time interval $t \in (0, 750 \mu\text{s})$, an increasing number of particles move upward as a consequence of the explosion taking place in $t \in (0, 500 \mu\text{s})$. The corresponding shock causes jamming and, thus, large pressure to the vertical walls enabling a large vertical force acting on the barrel. Accordingly, the barrel is accelerated upwards during this interval of time. Figure 9 (red line) shows the vertical velocity of the barrel which increases up to $t \approx 0.8$ ms. The formation of the solid plug leads to back-scattering of particles hitting the plug from below. Subsequently, such particles lead to *downward* acceleration of the barrel via collisions with the bottom or the side walls of the container, thus, reducing its upwards velocity. At approximately the same time, the plug quickly decays and the accelerating force ceases. At $t \approx 2.5$ ms, most of the ping-pong balls have left the container so that its motion follows essentially a ballistic trajectory under the action of gravity, perturbed only by a small number of random collisions with balls that are still inside the barrel. At this time, the barrel's upward terminal velocity is about 4 m/s, in nice agreement with the experiment.

The scenario described can be seen in Fig. 9 in good agreement with the visual impression of the movie provided in the Supplemental Material.³² At first glance, the values of the force density shown in Fig. 8 seem to be large, therefore, let us see whether the values are plausible: Consider the interval $t \in (500, 700) \mu\text{s}$ (green line) where significant forces act in the interval $z \in (0.15, 0.45)$ m. The gain of vertical velocity of the barrel during this interval of time is $\Delta v = \frac{F}{m} \Delta t \approx \frac{3 \cdot 10^5 \text{ N/m} \cdot 0.3 \text{ m}}{1.7 \text{ kg}} \cdot 2.5 \cdot 10^{-4} \text{ s} \approx 13.2 \text{ m/s}$ which is in good agreement with the gain of velocity of the barrel shown in Fig. 9 (green time interval). Therefore, the force density

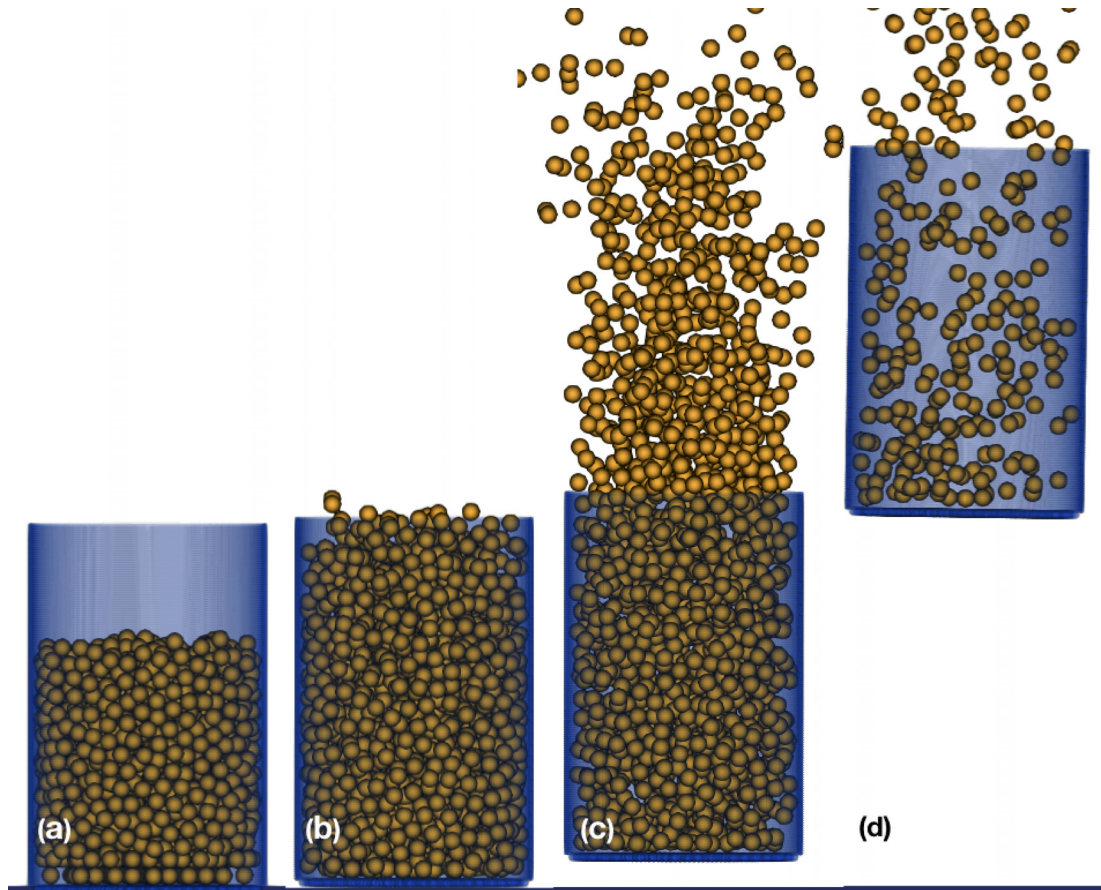


Fig. 6. Simulation of the flying barrel effect. (a) Initial state, $t=0$, just before the explosion; (b) $t=5$ ms, particles start leaving the barrel; (c) $t=20$ ms, the barrel becomes airborne and the particles are expelled at high velocity from the barrel; (d) $t=300$ ms, the barrel follows a ballistic trajectory mainly without interaction with the ping-pong balls, except for a few random collisions. An animated sequence of the process is provided as Supplemental Material (Ref. 32).

of typically $3 \times 10^5 \text{ N/m}$ (see Fig. 8) is plausible. In the simulations we used the friction coefficient $\mu=0.8$, therefore, the corresponding normal force density is $3.75 \times 10^5 \text{ N/m}$. But can ping-pong balls withstand these forces? The diameter of the barrel corresponds to the circumference $u \approx \pi \cdot 0.5 \text{ m}$, therefore, the pressure acting to the vertical wall is $3.75 \cdot 10^5 / (\pi \cdot 0.5) \text{ N/m}^2 \approx 2.4 \times 10^4 \text{ N/m}^2$, in the region of maximal pressure. The number density of disks of diameter d in hexagonal packing is $(\pi/\sqrt{12})/d^2 \approx 698/\text{m}^2$ where the size of a ping-pong ball was used. Thus, the average normal force exerted by a ball to the wall is approximately 343 N. This is a large force but significantly smaller than the maximal force the ball experiences during a professional ping-pong game. While a ping-pong ball cannot withstand a static load of this size it can stand short pulses of large amplitude without harm.³³

IV. SIMULATIONS WITH IDEALIZED CONDITIONS

In Sec. III, we presented numerical results to support our hypothesis concerning the physical origin of the flying-barrel effect, namely, an interplay between jamming of the ping-pong balls and friction. We can further corroborate the hypothesis by performing simulations where either the jamming or the transfer of momentum from the particles to the barrel due to friction is suppressed. While it would be difficult to investigate these situations experimentally, numerical simulations allow such experiments to be performed without difficulties.

For the first test, we consider ideally smooth particles which do not exert friction forces on each other. For frictionless particles, jamming is not observed with the exception of very small systems where the confinement is not larger than a few particle diameters. Consequently, the flying-barrel effect should not occur for ideally smooth spheres. This can be checked by a numerical simulation which agrees in all details with the description above, except that the friction coefficient $\mu=0$ was used for particle-particle contacts. Figure 9 (black line) shows the corresponding vertical velocity of the barrel as a function of time. Except for small oscillations due to the particle-wall contacts there is no significant motion of the barrel when jamming is suppressed.

Likewise, for ideally smooth barrel-particle contact no barrel jumping can be expected because no vertical friction force acts on the barrel, see Fig. 9 (blue line). The oscillation of small amplitude in the interval $t \in [5, 6] \times 10^{-4} \text{ s}$ results from the residual bumpiness of the barrel's surface, whose flat walls are modeled by many small overlapping spheres.

The interrelation between momentum exchange and friction can be worked out by a further modification of our numerical experiment: We remove the solid floor and perform the experiment under conditions of weightlessness by setting $g=0$. Unlike the original experiment where the solid floor supplies an *external* force onto the barrel, this setup preserves the total momentum. Figure 10 shows the momenta of the abundance of ping-pong balls and the barrel as functions of time.

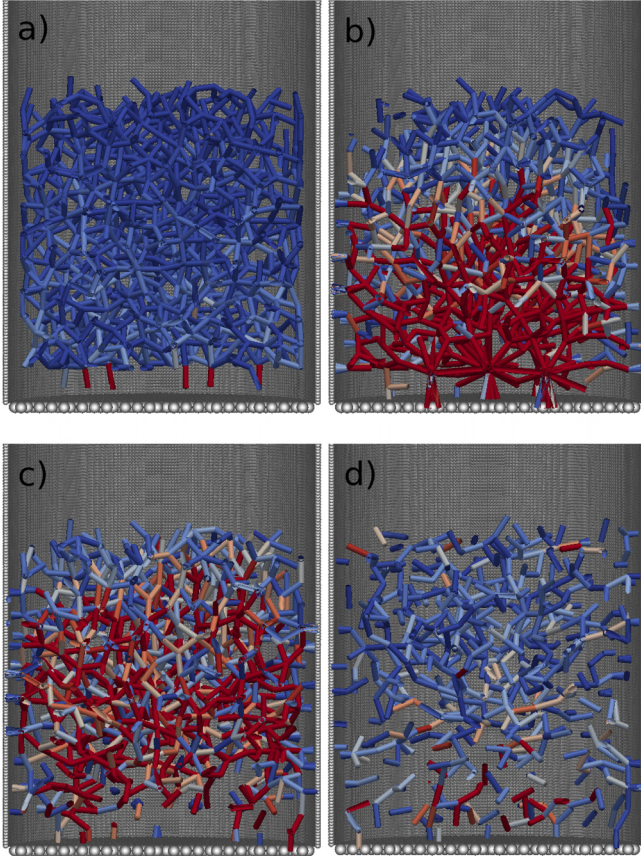


Fig. 7. Process of jamming represented by the evolution of the force network among the ping-pong balls. The center of each particle experiencing a contact force from one of its neighbors or from the wall is connected by a link representing the magnitude of the force in shear direction. (a) Initial state at $t=0$. Particles rest inside the barrel under the action of gravity (b) at $t=500 \mu\text{s}$, the shock due to the explosion of the bottle is fully developed and sustains large shear forces. (c) The shock reaches the top layer at $t \approx 650 \mu\text{s}$ and the plug decays. (d) $t=1$, 1 ms. An animated sequence is provided as Supplemental Material (Ref. 32).

For frictional particles, Fig. 10(a), the explosion initially causes the balls and the barrel to accelerate in opposite directions. This acceleration vanishes at the end of the explosion, $t \approx 5 \times 10^{-4}$ s, when the relative velocity of the balls and the barrel reaches its maximum. In the same interval of time, a plug of particles is formed by jamming, enabling large normal forces between the balls and the side wall of the barrel. This normal force, in turn, allows large friction forces between the plug of balls and the barrel moving in opposite directions. The resulting total friction force, thus, reduces the momentum difference between the balls and the barrel reaching a plateau at $t \approx 2$ ms. From this time on, the particles and the barrel move with nearly constant relative velocity, only perturbed by a small number of collisions between balls and the barrel.

For the case of frictionless interaction of balls and barrel shown in Fig. 10(b), the scenario is the same, except that the plug cannot exert frictional forces to the barrel due to Coulomb's law of friction. Therefore, after the explosion the relative momentum does not decrease but reaches a plateau at a larger value.

Comparing Figs. 10(a) and 10(b), we conclude that it is indeed the rapidly upward-moving plug of ping-pong balls which drags the barrel in the same direction. This behavior was counterintuitive when naively disregarding the process of jamming.

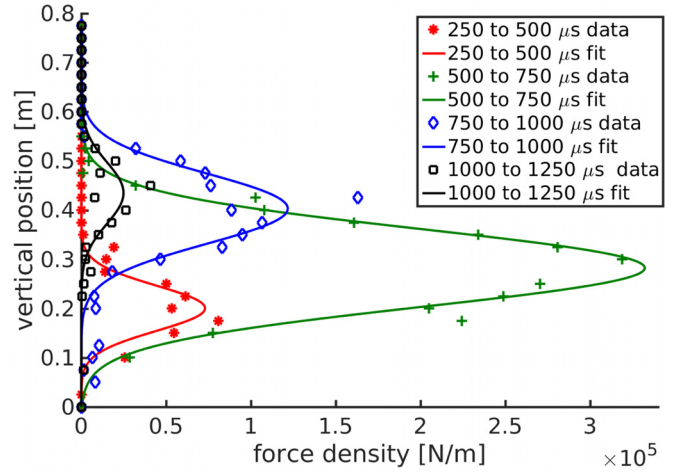


Fig. 8. Density of forces in the vertical direction between the particles and the barrel for different times after the explosion. The continuous lines show fits to Gaussian functions as a guide to the eye. In the course of time, the magnitude of forces accelerating the barrel upwards increases due to the explosion and later decreases when the shock arrives at the top layer of particles where the plug decays.

V. CONCLUSION

The counterintuitive effect of the barrel jumping in the same direction as the ping-pong balls was successfully recreated through numerical simulations and explained by a combination of the familiar granular jamming effect together with Coulomb friction between the plug of ping-pong balls and the vertical wall of the barrel. The force chain development and subsequent increase in contact forces is clearly captured in the instants that follow the explosion, indicating the formation of a stable structure. This structure is capable of sustaining vertical forces for a short period of time, but enough to significantly accelerate the barrel vertically. The force network is subsequently dissipated, allowing the balls to escape the barrel. No jumping-barrel effect could be seen when either the formation of the plug or the friction between the plug and the barrel is suppressed by choosing the friction

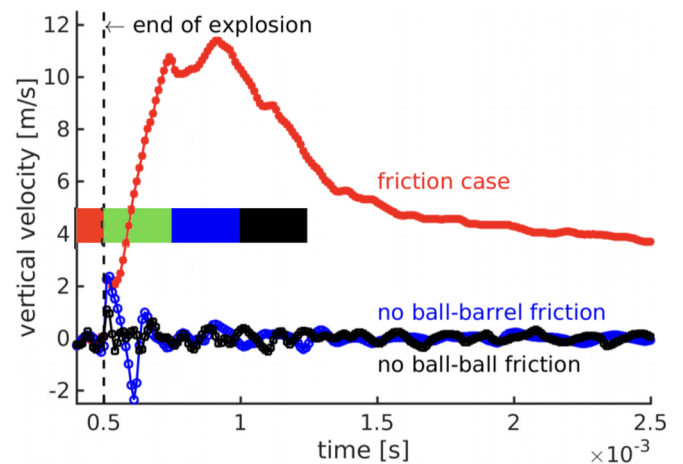


Fig. 9. Vertical barrel velocity as a function of time (friction case; for explanation see the text). No ball-ball friction line: same as the friction case but for frictionless particle-particle interaction, when jamming is inhibited. No ball-ball friction line: same, but for frictionless particle-barrel interaction. The horizontal bar marks the corresponding time intervals used for averaging of the forces shown in Fig. 8. For animated sequences see Supplemental Material (Ref. 32).

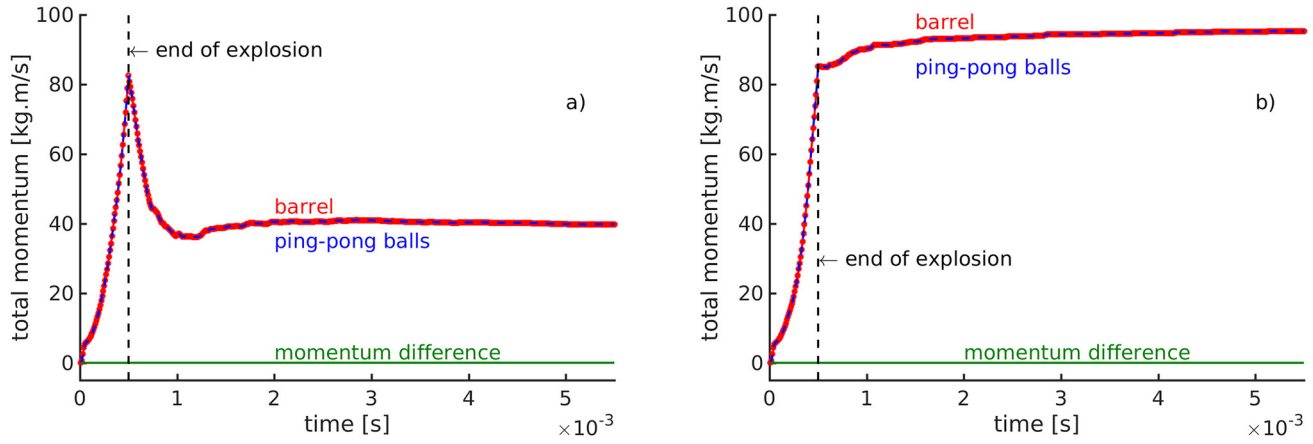


Fig. 10. Experiment under conditions of weightlessness. Momenta of the abundance of ping-pong balls (dashed line) and the barrel (continuous line) and the difference of both (constant horizontal line). For better comparison of the data, the momentum of the barrel is drawn with negative sign. (a) Standard setup without the solid floor; (b) same but for frictionless interaction of the ball-barrel contacts, $\mu = 0$. For animated sequences see Supplemental Material (Ref. 32).

coefficient $\mu = 0$. In the numerical simulations using realistic material and system parameters, the barrel jumps to a height of approximately 0.9 m which is in good agreement with most nitrogen and ping-pong balls experiments available on the internet.

The results presented here demonstrate the usefulness of numerical simulations for understanding physical phenomena at limits at which experimental verification can be hard to perform. For instance, switching off (or drastically reducing) friction and/or gravity to study the interplay of jamming and friction while experimentally feasible, certainly involve much larger efforts.

ACKNOWLEDGMENTS

The authors thank Professor Roy Lowry for providing high-resolution footage of Figs. 1 and 4. The authors acknowledge funding by the German Research Foundation (Deutsche Forschungsgemeinschaft) through the Cluster of Excellence “Engineering of Advanced Materials,” ZISC, FPS and Grant No. RI2497/6-1. J.A.C.G. was also supported by CNPq, Brazil.

APPENDIX: SIMULATION METHOD

The ping-pong balls as well as the barrel considered here are both macroscopic objects whose dynamics may be described by classical mechanics, that is, if all acting forces are known, the temporal evolution of the system is given by Newton’s equations of motion. We solve this set of ordinary differential equations to simulate the dynamics of the ping-pong balls and the barrel. This method is often referred to as the discrete element method (DEM).^{34,35}

To obtain the interaction forces needed for a DEM simulation, we model the ping-pong balls and the balls that constitute the barrel as deformable spheres. When the ping-pong spheres collide they mutually deform each other. The deformation can be quantified by

$$\xi \equiv \max[0, R_i + R_j - r], \quad (\text{A1})$$

where $r \equiv |\vec{r}|$ is the absolute value of the inter-center relative vector $\vec{r} \equiv \vec{r}_j - \vec{r}_i$. A representation of the colliding spheres and the corresponding stages of the collision is shown in Fig. 11.

The deformation causes an interaction force, \vec{F} , that is, in the contact point the force \vec{F} acts on particle i and the force $-\vec{F}$ on particle j , respectively. It is convenient to subdivide the interaction force \vec{F} in a part \vec{F}_n parallel and a part \vec{F}_t perpendicular to the inter center vector \vec{r}

$$\vec{F} = \vec{F}_n + \vec{F}_t, \quad (\text{A2})$$

$$\vec{F}_n = (\vec{F} \cdot \hat{e}_n) \equiv F_n \hat{e}_n, \quad (\text{A3})$$

$$\vec{F}_t = \vec{F} - \vec{F}_n \equiv F_t \hat{e}_t, \quad (\text{A4})$$

where $\hat{e}_n \equiv \vec{r}/r$ is the inter center unit vector.

For viscoelastic spheres, F_n is given by

$$F_n = F^{\text{el}} + F^{\text{dis}} = \rho_{\text{el}} \xi^{3/2} - \frac{3}{2} A_{\text{dis}} \rho_{\text{el}} \dot{\xi} \sqrt{\xi}, \quad (\text{A5})$$

with

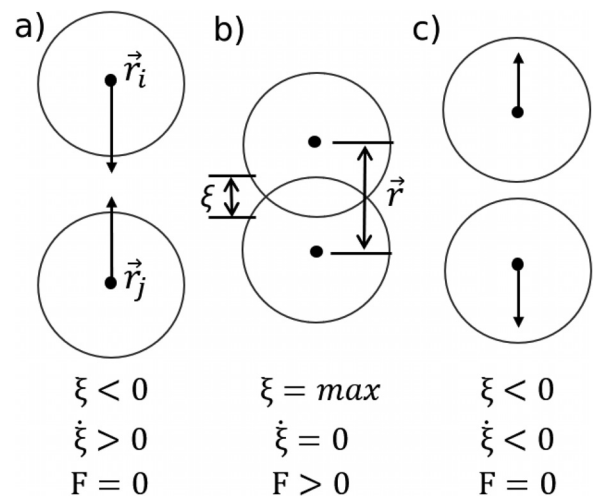


Fig. 11. Sequential representation of two spheres colliding. (a) Spheres approach one another at relative velocity $\dot{\xi}$. (b) Particles collide and deform one another by ξ . This deformation corresponds to a repulsive force, decelerating the relative motion. When the compression assumes its maximum (repulsive force also assumes its maximum), the relative velocity ceases. In (c), the particles are no longer in contact and the repulsive force vanishes.

$$\rho_{\text{el}} \equiv \frac{2Y\sqrt{R_{\text{eff}}}}{3(1-\nu^2)}, \quad (\text{A6})$$

where Y , ν , and R_{eff} denote the Young's modulus, the Poisson's ratio, and the effective radius $R_{\text{eff}} = R_i R_j / (R_i + R_j)$, respectively. If two spheres of different materials collide, the term $Y/(1-\nu^2)$ in Eq. (A6) has to be replaced by

$$Y_{\text{eff}} \equiv \frac{Y_i Y_j}{(1-\nu_i^2)Y_j + (1-\nu_j^2)Y_i}, \quad (\text{A7})$$

where Y_{ij} and ν_{ij} are the Young's modulus and Poisson's ratio of particle i and j .³⁶ The elastic part, F^{el} , of this widely used collision model is given by the Hertz contact force³⁷ and the dissipative part, F^{dis} , corresponds to linear viscoelasticity of the particle material.³⁸ The dissipative part in the force model (A5) may overcompensate the elastic restoring force, leading to an unphysical attractive interaction force. Therefore, F_n has to be limited to $F_n = \max(0, F^{\text{el}} + F^{\text{dis}})$, which corresponds to a premature end of the collision where the particles detach while still deformed and recover their spherical shape only after the collision has ceased.

At the contact point, the relative velocity \vec{v} between the surfaces of two colliding spheres reads

$$\vec{v} \equiv (\dot{\vec{r}}_j - \dot{\vec{r}}_i) + \hat{e}_n \times (R_i \vec{\omega}_i + R_j \vec{\omega}_j), \quad (\text{A8})$$

where $\vec{\omega}_i$ and $\vec{\omega}_j$ denote the angular velocities of particles i and j , respectively. Similar to the treatment of the interaction force, we decompose this velocity into a component, \vec{v}_n , parallel and a component, \vec{v}_t , perpendicular to the inter-center unit-vector \hat{e}_n

$$\vec{v}_n = (\vec{v} \cdot \hat{e}_n) \hat{e}_n \equiv v_n \hat{e}_n, \quad (\text{A9})$$

$$\vec{v}_t = \vec{v} - \vec{v}_n \equiv v_t \hat{e}_t. \quad (\text{A10})$$

The coefficient of restitution relates the normal components of the pre- and post-collisional relative velocity (v_n and v'_n) between the colliding particles

$$\varepsilon \equiv -\frac{v'_n}{v_n}. \quad (\text{A11})$$

For the interaction force (A5), ε can be computed analytically as a function of the material parameters and the impact velocity.³⁹⁻⁴² For a given coefficient of restitution, this relation may in turn be used to compute the dissipative parameter A_{dis} in Eq. (A5). In our simulations, the typical impact velocity is $v_{\text{char}} \approx 120$ m/s in the explosion phase where all relevant collisions occur. We choose A_{dis} such that the resulting coefficient of restitution is $\varepsilon = 0.8$ for the typical impact velocity v_{char} .

For the tangential part, F_t , of the interaction force (see Eq. (A4)) we use the model by Cundall and Strack.⁴³ Here, it is assumed that particles moving at tangential relative velocity, v_t while being in contact, load a spring. The spring is initialized at the time t_c when the particles get into contact and it exists until the particle surfaces separate from each other

$$\zeta(t) \equiv \int_{t_c}^t v_t(t^*) dt^*. \quad (\text{A12})$$

The tangential force is then proportional to the deformation of the spring, ζ , again limited by Coulomb's law

$$F_t = -\text{sign}(v_t) \cdot \min(|\kappa \zeta|, \mu |F_n|), \quad (\text{A13})$$

where μ is the coefficient of friction and κ is the elastic constant of the spring. This widely used model is related to the normal elastic force through the Poisson's ratio, shear modulus and Young's modulus relation.⁴⁴ Here we used $\kappa = 0.467\rho_{\text{el}}$.

For hollow gas-filled ping-pong balls, it is known that the repulsive interaction force is a complicated function of the mutual deformation and the relative velocity. This is true even for the simplest case of a ball impacting a solid plane.³³ For balls which are in contact with more than one other object, that is, another ball or a plane, the interaction will be even more complex. Therefore, the application of the interaction force model presented, assuming homogeneous viscoelastic material for the ping-pong balls, is certainly questionable. However, to our knowledge, no interaction force model for hollow gas-filled balls is available in the literature. Therefore, for the simulation presented here, we adopted simplifying assumptions for the interaction force and checked, that the presented results do not qualitatively depend on the concrete choice of the interaction force. That is, when using other force laws, we obtain qualitatively similar results.

The numerical integration of Newton's equation of motion using the described interaction force was performed with the open source software LIGGGHTS.⁴⁵

¹Sick Science Youtube Channel, "Liquid nitrogen ping pong ball explosion on the Ellen show," <<https://www.youtube.com/watch?v=Jh5Y8Gb-kFU>>.

²Alan Williams and Roy Lowry, "Liquid nitrogen and ping-pong balls collide," <<https://www.plymouth.ac.uk/news/liquid-nitrogen-and-ping-pong-balls-collide-in-the-name-of-science>> (2015).

³Roy Lowry, "Slow motion ping-pong ball explosion," <<https://www.youtube.com/watch?v=sjPl3EXLb2Y>>.

⁴Isaac Newton, *Philosophiæ Naturalis Principia Mathematica* (Jussu Societatis Regiæ ac typis Josephi Streater, London, 1687).

⁵See <<https://io9.gizmodo.com/scientist-liquid-nitrogen-1500-ping-pong-balls-bo-5944687>> for a description of this experiment and discussions related to the physics behind the experiment.

⁶See <<https://physics.stackexchange.com/questions/38494/whats-driving-the-bucket-up>> for a physics related forum topic debating on why the barrel flies in the same direction as the ping pong balls in the current experiment.

⁷See <<https://forums.parallax.com/discussion/142686/liquid-nitrogen-1500-ping-pong-balls>> for a forum topic discussing the many phenomena related to this experiment.

⁸Noble Research Institute Youtube Channel, "Huge liquid nitrogen explosion," <<https://www.youtube.com/watch?v=wryjzi9sdBg>>.

⁹Youtube Video, "Liquid nitrogen and hot water," <https://www.youtube.com/watch?v=gCD7WFMTH_k>.

¹⁰Youtube Video, "Liquid nitrogen + Warm soap water," <<https://www.youtube.com/watch?v=6Tdb9WcKzGA>>.

¹¹Distort Youtube Channel, "Ping pong ball explosion with liquid nitrogen in slow motion," <<https://www.youtube.com/watch?v=Gsxpt1etTnA>>.

¹²Florian Freistetter, "Flüssiger Stickstoff + 1500 Tischtennisbälle = Coolness," <<http://scienceblogs.de/astrodicticum-simplex/2012/09/21/fluessiger-stickstoff-1500-tischtennisballe-coolness/>> (2012).

¹³Andrea J. Liu and Sidney R. Nagel, "Jamming is not just cool any more," *Nature* **396**, 21–22 (1998).

¹⁴Giulio Biroli, "A new kind of phase transition?," *Nat. Phys.* **3**, 222–223 (2007).

¹⁵*Jamming and Rheology: Constrained Dynamics on Microscopic and Macroscopic Scales*, edited by Andrea J. Liu and Sidney R. Nagel (Taylor & Francis, London, New York, 2001).

¹⁶Thorsten Pöschel, "Recurrent clogging and density waves of granular material flowing in a narrow pipe," *J. Phys. I. France* **4**, 499–506 (1994).

¹⁷Iker Zuriguel, Angel Garcimartín, Diego Maza, Luis A. Pugnaloni, and J. M. Pastor, "Jamming during the discharge of granular matter from a silo," *Phys. Rev. E* **71**, 051303 (2005).

- ¹⁸Alexandre Nicolas, Ángel Garcimartín, and Iker Zuriguel, “Trap model for clogging and unclogging in granular hopper flows,” *Phys. Rev. Lett.* **120**, 198002 (2018).
- ¹⁹Thorsten Pöschel and Volkhard Buchholtz, “Molecular dynamics of arbitrarily shaped granular particles,” *J. Phys. I France* **5**, 1431–1455 (1995).
- ²⁰Bulbul Chakraborty and Robert P. Behringer, *Jamming of Granular Matter* (Springer, NY, 2009), pp. 4997–5021.
- ²¹Hu Zheng, Dong Wang, Jonathan Barés, and Robert P. Behringer, “Sinking in a bed of grains activated by shearing,” *Phys. Rev. E* **98**, 010901 (2018).
- ²²Raúl C. Hidalgo, Balázs Szabó, Katalin Gillemot, Tamas Börzsönyi, and Thomas Weinhart, “Rheological response of nonspherical granular flows down an incline,” *Phys. Rev. Fluids* **3**, 074301 (2018).
- ²³Abram H. Clark, Jacob D. Thompson, Mark D. Shattuck, Nicholas T. Ouellette, and Corey S. O’Hern, “Critical scaling near the yielding transition in granular media,” *Phys. Rev. E* **97**, 062901 (2018).
- ²⁴Dong Wang, Jie Ren, Joshua A. Dijksman, Hu Zheng, and Robert P. Behringer, “Microscopic origins of shear jamming for 2d frictional grains,” *Phys. Rev. Lett.* **120**, 208004 (2018).
- ²⁵Adrian Baule, Flaviano Morone, Hans J. Herrmann, and Hernán A. Makse, “Edwards statistical mechanics for jammed granular matter,” *Rev. Mod. Phys.* **90**, 015006 (2018).
- ²⁶Tino Riethmüller, Lutz Schimansky-Geier, Dirk Rosenkranz, and Thorsten Pöschel, “Langevin equation approach to granular flow in a narrow pipe,” *J. Stat. Phys.* **86**, 421–430 (1997).
- ²⁷Yann Bertho, Frédérique Giorgiutti-Dauphiné, Tarek Raafat, E. John Hinch, Hans-Jürgen Herrmann, and Jean-Pierre Hulin, “Powder flow down a vertical pipe: The effect of air flow,” *J. Fluid Mech.* **459**, 317–345 (2002).
- ²⁸Carlos A. Alvarez and Erick de Moraes Franklin, “Intermittent gravity-driven flow of grains through narrow pipes,” *Physica A* **465**, 725–741 (2017).
- ²⁹Jochen Schäfer and Dietrich Wolf, “Transients in homogeneous granular pipe flow,” in *Workshop on Traffic and Granular Flow: HLRZ, Forschungszentrum Jülich, Germany*, October 9–11 1995, edited by Dietrich Wolf, Michael Schreckenberg, and Achim Bachem (World Scientific, Singapore (u.a.), 1996), p. 347.
- ³⁰Felix Verbücheln, Eric J. R. Parteli, and Thorsten Pöschel, “Helical inner-wall texture prevents jamming in granular pipe flows,” *Soft Matter* **11**, 4295–4305 (2015).
- ³¹Roy Lowry, “A liquid nitrogen bomb mixed with 1500 ping pong balls,” <<https://www.youtube.com/watch?v=mxwPfwy878>> (2012).
- ³²See supplementary material at <https://doi.org/10.1119/1.5088805> for animated sequences of the simulation Movie M1.mp4 shows a numerical simulation of the ping-pong balls cannon. In quantitative agreement with the experiment, the barrel jumps to a height of approximately 0.9 m. Movie M2.mp4 shows the formation of the force network (plug formation) during the first 600 μ s after the beginning of the explosion and its later decay. The left side shows a cut through the barrel and details of the modeling of the explosion. The force network is shown right where the forces are represented by bars whose color codes the shear forces. The movie therefore shows the vertical forces transmitted between ping-pong balls in contact with the barrel responsible for the acceleration of the barrel. Movie M3.mp4 shows a numerical simulation of idealized systems where either the friction between ping-pong balls (left) or the friction between ping-pong balls and the barrel (right) is omitted. The first case suppresses jamming, the second case does not allow transfer of momentum in the vertical direction between the plug and the barrel. In both cases the barrel remains in contact with the floor while the ping-pong balls leave the barrel at high velocity. Movie M4.mp4 shows a numerical simulations of the system in the absence of gravity and a solid floor. In this case, the total momentum is conserved due to the absence of external forces. Left: frictional walls and frictional particles; right: no friction at the wall. In the latter case, the terminal relative velocity between the center of mass of the balls and the barrel is smaller since friction between the plug of particles and the vertical walls decelerates the relative motion; <<https://mss.cbi.fau.de/sup/ping-pong-cannon/>>.
- ³³Rod Cross, “Impact behavior of hollow balls,” *Am. J. Phys.* **82**, 189–195 (2014).
- ³⁴Thorsten Pöschel and Thomas Schwager, *Computational Granular Dynamics: Models and Algorithms* (Springer, Berlin, Heidelberg, New York, 2010).
- ³⁵Hans-Georg Matuttis and Jian Chen, *Understanding the Discrete Element Method: Simulation of Non-Spherical Particles for Granular and Multi-body Systems* (Wiley, Singapore, 2005).
- ³⁶Thorsten Pöschel and Thomas Schwager, *Computational Granular Dynamics* (Springer Berlin Heidelberg, Heidelberg, 2005).
- ³⁷Heinrich Hertz, “Über die Berührung fester elastischer Körper,” *J. f. reine u. Angewandte Math.* **92**, 156–171 (1882).
- ³⁸Nikolai V. Brilliantov, Frank Spahn, Jan-Martin Hertzsch, and Thorsten Pöschel, “Model for collisions in granular gases,” *Phys. Rev. E* **53**, 5382–5392 (1996).
- ³⁹Thomas Schwager and Thorsten Pöschel, “Coefficient of normal restitution of viscous particles and cooling rate of granular gases,” *Phys. Rev. E* **57**, 650–654 (1998).
- ⁴⁰Rosa Ramírez, Thorsten Pöschel, Nikolai V. Brilliantov, and Thomas Schwager, “Coefficient of restitution of colliding viscoelastic spheres,” *Phys. Rev. E* **60**, 4465–4472 (1999).
- ⁴¹Thomas Schwager and Thorsten Pöschel, “Coefficient of restitution for viscoelastic spheres: The effect of delayed recovery,” *Phys. Rev. E* **78**, 051304 (2008).
- ⁴²Patric Müller and Thorsten Pöschel, “Collision of viscoelastic spheres: Compact expressions for the coefficient of normal restitution,” *Phys. Rev. E* **84**, 021302 (2011).
- ⁴³Peter A. Cundal and Otto D. L. Strack, “A discrete numerical model for granular assemblies,” *Géotechnique* **29**, 47–65 (1979).
- ⁴⁴Alberto Di Renzo and Francesco Di Maio, “An improved integral non-linear model for the contact of particles in distinct element simulations,” *Chem. Eng. Sci.* **60**, 1303–1312 (2005).
- ⁴⁵Christoph Kloss, Christoph Goniva, Alice Hager, Stefan Amberger, and Stefan Pirker, “Models, algorithms and validation for opensource DEM and CFD-DEM,” *Prog. Comp. Fluid Dyn.* **12**, 140–152 (2012).